RESEARCH ARTICLE

Movement of IS*26*-Associated Antibiotic Resistance Genes Occurs via a Translocatable Unit That Includes a Single IS*26* and Preferentially Inserts Adjacent to Another IS*26*

Christopher J. Harmer, Robert A. Moran, Ruth M. Hall

School of Molecular Bioscience, The University of Sydney, Sydney, Australia

ABSTRACT **The insertion sequence IS*26* plays a key role in disseminating antibiotic resistance genes in Gram-negative bacteria, forming regions containing more than one antibiotic resistance gene that are flanked by and interspersed with copies of IS*26*. A model presented for a second mode of IS*26* movement that explains the structure of these regions involves a translocatable unit consisting of a unique DNA segment carrying an antibiotic resistance (or other) gene and a single IS copy. Structures resembling class I transposons are generated via RecA-independent incorporation of a translocatable unit next to a second IS*26* such that the ISs are in direct orientation. Repeating this process would lead to arrays of resistance genes with directly oriented copies of IS*26* at each end and between each unique segment. This model requires that IS*26* recognizes another IS*26* as a target, and in transposition experiments, the frequency of cointegrate formation was 60-fold higher when the target plasmid contained IS*26*. This reaction was conservative, with no additional IS*26* or target site duplication generated, and orientation specific as the IS*26*s in the cointegrates were always in the same orientation. Consequently, the cointegrates were identical to those formed via the known mode of IS*26* movement when a target IS*26* was not present. Intact transposase genes in both IS*26*s were required for high-frequency cointegrate formation as inactivation of either one reduced the frequency 30-fold. However, the IS*26* target specificity was retained. Conversion of each residue in the DDE motif of the Tnp26 transposase also reduced the cointegration frequency.**

IMPORTANCE **Resistance to antibiotics belonging to several of the different classes used to treat infections is a critical problem. Multiply antibiotic-resistant bacteria usually carry large regions containing several antibiotic resistance genes, and in Gram-negative bacteria, IS*26* is often seen in these clusters. A model to explain the unusual structure of regions containing multiple IS*26* copies, each associated with a resistance gene, was not available, and the mechanism of their formation was unexplored. IS*26*-flanked structures deceptively resemble class I transposons, but this work reveals that the features of IS*26* movement do not resemble those of the IS and class I transposons studied to date. IS*26* uses a novel movement mechanism that defines a new family of mobile genetic elements that we have called "translocatable units." The IS*26* mechanism also explains the properties of IS*257* (IS*431*) and IS*1216*, which belong to the same IS family and mobilize resistance genes in Gram-positive staphylococci and enterococci.**

Received 1 September 2014 **Accepted** 12 September 2014 **Published** 7 October 2014

Citation Harmer CJ, Moran RA, Hall RM. 2014. Movement of IS*26*-associated antibiotic resistance genes occurs via a translocatable unit that includes a single IS*26* and preferentially inserts adjacent to another IS*26*. mBio 5(5):e01801-14. doi:10.1128/mBio.01801-14.

Editor Karen Bush, Indiana University, Bloomington

Address correspondence to Ruth M. Hall, ruth.hall@sydney.edu.au.

This article is a direct contribution from a Fellow of the American Academy of Microbiology.

IS*26*, which was first described over three decades ago (1), is a member of the IS*6* family (2), and IS*26* may be identical to IS*6*, which has never been sequenced. IS*26* was present in many early antibiotic-resistant isolates and was given several other names: IS*15*Δ, IS*46*, IS*140*, IS*160*, IS*176*, and IS*1936* (3–8). However, these ISs are now known to be identical (3, 9). IS*26* plays a critical role in the dissemination of antibiotic resistance genes in Gram-negative bacteria, as it is associated with genes conferring resistance to many different classes of antibiotics (for example, see references 7, 8, and 10–20) or partial class 1 integrons (21). IS*26* is known to be able to contribute to the expression of the associated resistance gene by supplying a promoter −35 box that can be coupled with a −10 in the adjacent DNA (14, 22).

Antibiotic resistance genes flanked by IS*26*s resemble class I or composite transposons, which consist of two ISs flanking a central segment. In most cases, the IS*26*s are in a direct orientation. However, structures containing more than two IS*26*s exhibit a feature that is not consistent with this designation because they include multiple putative composite transposons (IS*26*-unique segment-IS*26*) in an array that contains too few copies of the IS (11). That is, the adjacent putative transposons share a single IS*26* located between them. An example of two overlapping IS*26*-bounded structures, each of which is also found alone, has been found in several locations (11). Further examples of these arrays are found in many complex regions containing several different antibiotic resistance genes (for examples, see references 11, 15, and 23–25). The arrangement is shown schematically in Fig. 1A. This configuration cannot be explained if the individual "transposons" move in the

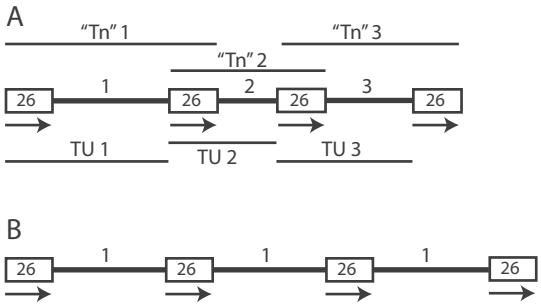

FIG 1 Configuration of regions containing multiple copies of IS*26*. (A) Different IS*26*-flanked DNA segments clustered, with insufficient copies of IS*26* for the unit of mobilization to be a typical class I transposon. IS*26*s are represented as boxes with a horizontal arrow indicating the position and orientation of *tnp26*. Thick horizontal lines with numbers above denote different segments of DNA. The extents of potential overlapping transposon forms ("Tn") are indicated above, and hypothetical translocatable units (TU) are shown below. (B) A single IS*26*-flanked DNA segment in a multimeric array.

same way as the well-studied composite transposons Tn*5* and Tn*10* (26, 27), which move as a single discrete unit. Duplication of IS*26*-flanked structures detected after the selective pressure of antibiotic use has also been reported, and this leads to the formation of tandem arrays (Fig. 1B) of the same DNA fragment interspersed with directly oriented copies of IS*26* (28–31).

IS*26* (Fig. 2) is 820 bp long, with 14-bp perfect terminal inverted repeats and a single gene, *tnp26*, that encodes a transposase (Tnp26) of 234 amino acids (aa) (1). IS*26* has been shown to form a cointegrate between the DNA molecule it resides in and the target molecule, but whether transposition via a cut-and-paste mechanism can also occur has not been investigated. In cointegrates, the IS*26* is duplicated, resulting in two copies of IS*26* in direct orientation, one at each boundary between the two participating molecules. Transposition generates an 8-bp duplication of the target site, which is found flanking the incoming molecule (32, 33). IS*15* and IS*15*Δ have been shown to function in the same manner (34, 35). In these studies, resolution of cointegrates was only seen in strains that were proficient for homologous recombination.

Despite the prevalence of IS*26* in the resistance gene clusters of antibiotic-resistant Gram-negative bacteria, transposition of IS*26* has not been further examined since the 1980s. Consequently, the mechanism behind IS*26*-mediated mobilization of resistance genes has not been explored. In order to better understand IS*26*-mediated mobilization of resistance genes in Gram-negative bacteria and the impact that it has on the evolution of multiple antibiotic resistance in bacterial populations, we have proposed a model to explain the structures observed. A standard conduction assay was then used to experimentally demonstrate that IS*26* movement exhibits some of the properties predicted by this model.

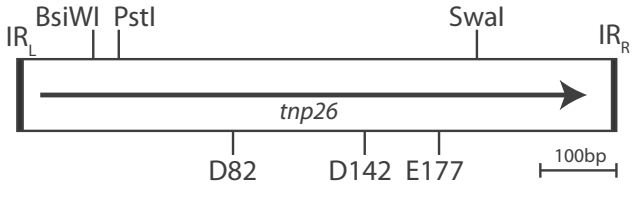

FIG 2 IS*26* schematic. The horizontal arrow shows the position and orientation of *tnp26*. Short vertical lines indicate the locations of the conserved amino acids in the DDE triad, and longer vertical lines indicate the locations of restriction sites. IR$_L$ and IR$_R$ mark the IS*26* left and right inverted repeats, respectively.

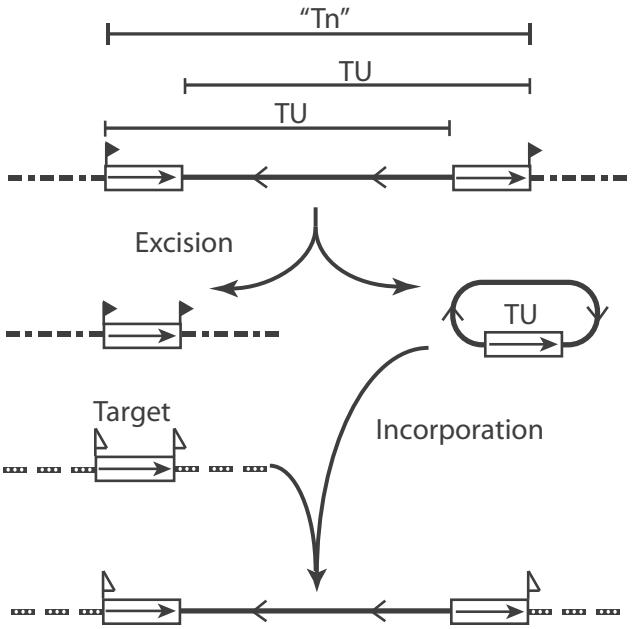

FIG 3 Mechanism of IS*26* mobilization. IS*26*s are shown as open boxes, with an arrow indicating the position and orientation of *tnp26*. Arrows give orientation to the central gene fragment. Flags indicate the position and direction of duplications formed from the insertion of IS*26*.

RESULTS

Model for movement of IS*26*-associated DNA segments containing antibiotic resistance genes. To account for the observed structures with an IS*26* shared between two adjacent apparent class I transposons and for the formation of tandem arrays shown in Fig. 1, we propose the model shown in Fig. 3 in which the unit of mobility is a single copy of the IS together with a unique DNA segment. To clearly distinguish this unit from a class I transposon, we will call it a "translocatable unit" (TU). In the model, the IS*26* in the TU targets an existing copy of IS*26* and the TU is incorporated immediately adjacent to it without increasing the number of IS*26* copies or creating a further duplication of the target. This model predicts the preferential interaction of two IS*26*s and that the process is conservative (i.e., duplication of IS*26* and of the target site does not occur in this mode).

Movement of IS*26*. All experiments were conducted in a *recA* mutant *Escherichia coli* background to ensure that the events detected had been catalyzed by the IS*26*-encoded transposase Tnp26. First, the ability of a single copy of IS*26* to form cointegrates as described previously was confirmed using a mating-out assay to detect the cointegrates formed between the plasmid pRMH762 (which confers ampicillin resistance [Ap^r]), which contains a single IS*26*, and the conjugative plasmid R388 (which confers sulfonamide and trimethoprim resistance [Su^r Tp^r]) residing together in the *E. coli recA* mutant background. The Ap^r Tp^r transconjugants carrying cointegrates were detected at an average of 2.9×10^{-6} cointegrates per Tp^r transconjugant (Table 1). Digestion of several

TABLE 1 Transposition frequency of pRM762 and derivatives

Plasmid	IS*26*	Target	Transposition frequency[a]		
			Mean	No.[b]	Range
pRMH762	IS*26*	R388	2.9×10^{-6}	10	1.3×10^{-6}–5.1×10^{-6}
pRMH962	IS*26*-FS-L[c]	R388	$<1.9 \times 10^{-8}$	3	$<2.9 \times 10^{-9}$– $<5.4 \times 10^{-8}$
pRMH762	IS*26*	R388::IS*26*	1.8×10^{-4}	10	5.4×10^{-5}–4.7×10^{-4}
pRMH962	IS*26*-FS-L	R388::IS*26*	5.9×10^{-6}	3	5.8×10^{-6}–7.5×10^{-6}
pRMH762	IS*26*	R388::IS*26*-FS–R[d]	4.3×10^{-6}	3	3.9×10^{-6}–4.9×10^{-6}
pRMH962	IS*26*-FS-L	R388::IS*26*-FS–R	$<3.5 \times 10^{-9}$	3	$<2.4 \times 10^{-9}$– $<5.1 \times 10^{-9}$

[a] Transposition frequency expressed as cointegrates per transconjugant.
[b] Number of independent determinations.
[c] IS*26*-FS-L, frameshift mutation in pRMH762 IS*26* *tnp26*.
[d] IS*26*-FS–R, frameshift mutation in R388::IS*26* *tnp26*.

independent cointegrates with BglII and BsiWI mapped the location of the junctions between the two plasmids and showed that pRMH762 had incorporated randomly throughout the R388 backbone (Fig. 4). The precise boundaries between the two plasmids relative to one another were determined for 10 cointegrates using primers in the R388 backbone adjacent to the predicted cointegrate boundaries with primers internal to pRMH762 (RH1451 and RH1452) to amplify each boundary. Both orientations of the plasmids relative to one another were found. The sequence spanning each IS*26* revealed that a copy of IS*26* was found in direct orientation at each boundary, and a duplication of 8 bp of R388 had been generated.

To confirm the requirement for Tnp26, pRMH962 (Ap^r), a derivative of pRMH762 with a frameshift at the left end of the IS*26* transposase gene (BsiWI site in Fig. 2) that would truncate the 234-aa transposase to a 30-aa protein was also examined. Cointegrate formation between R388 and pRMH962 was not detected in three independent experiments (Table 1).

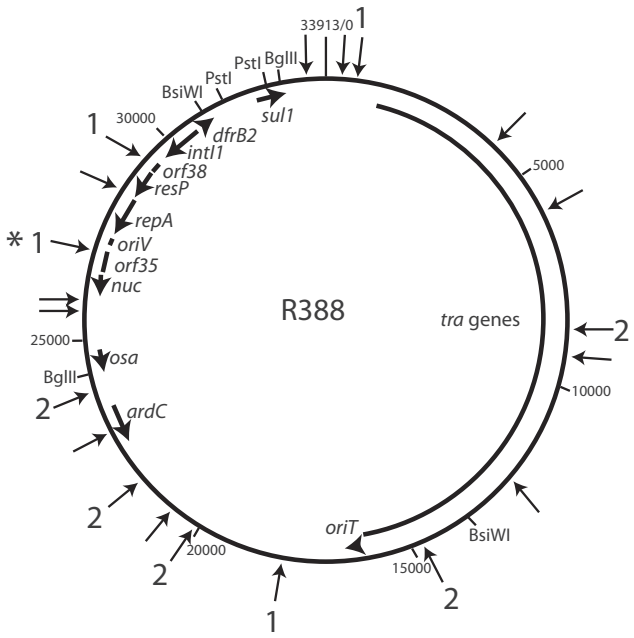

FIG 4 Cointegrate formation between pRMH762 and R388. The R388 backbone is drawn to scale from GenBank accession no. BR000038 with key resistance genes, genes involved in replication (*repA*), and genes involved in conjugative transfer (*tra*) shown as arrows inside the circular backbone. Arrows pointing toward the circular backbone indicate the location of 20 mapped R388::pRMH762 cointegrates. The precise location and orientation of nine cointegrates were determined by sequencing. An arrow labeled 1 indicates a cointegrate with *tnp26* facing clockwise, while an arrow labeled 2 indicates a cointegrate with *tnp26* facing counterclockwise. An asterisk denotes the cointegrate used in the construction of R388::IS*26*.

TUs target IS*26*. In the cointegration assay, the small plasmid carrying IS*26* can be viewed as a TU that has the capacity to replicate. To examine the prediction that when a second copy of IS*26* is present it acts as a preferred target, the conjugative plasmid was replaced with R388::IS*26* containing a single copy of IS*26*. The location of this IS is indicated by an asterisk in Fig. 4. Cointegrates formed between pRMH762 and R388::IS*26* were recovered at an average frequency of 1.78×10^{-4} per R388::IS*26* transconjugant (Table 1), and this represents a 60-fold increase in transposition frequency compared to when R388 was the target. Mapping of plasmid DNA extracted from 20 Ap^r Tp^r transconjugants (2 from each of 10 independent experiments) revealed that they all produced the same restriction pattern, and this corresponded to the pattern expected if incorporation of pRMH762 (the TU) had occurred adjacent to the IS*26* in R388::IS*26*.

The position of the cointegrate junctions was confirmed and the orientation determined using primer pairs RH1471/RH1452 and RH1472/RH1451 to link the R388 backbone across each IS*26* into the pRMH762-derived region (Fig. 5). PCR products of the expected size (1,464 bp and 1,042 bp, respectively) confirmed that all of the tested cointegrates shared the same boundaries between pRMH762 and R388::IS*26*, and the IS*26*s were always in the direct orientation. The sequences of the PCR amplicons showed that, in every case, the direct repeats flanking the single IS*26* in R388::IS*26* were now located next to the left and right ends of the IS*26*-flanked pRMH762 and the direct repeats surrounding the IS*26* in pRMH762 were at the internal boundaries (Fig. 5). Hence, the incorporation of pRMH762 adjacent to the IS*26* in R388::IS*26* did not generate an additional copy of IS*26* or a duplication of a target sequence (i.e., the reaction was conservative).

High-frequency recombination between two IS*26*s requires an active Tnp26 produced by both IS*26*s. To determine whether an active Tnp26 transposase must be produced by both copies of IS*26* participating in the reaction, cointegrate formation between R388::IS*26* and pRMH962 (with a frameshift in *tnp26*) was measured, and Ap^r Tp^r transconjugants were recovered at a frequency of 2.5×10^{-6}/Tp^r transconjugant (Table 1). This represents a 30-fold decrease in efficiency compared to when both IS*26*s are intact. However, restriction mapping of a cointegrate from each of five independent experiments produced the same restriction pat-

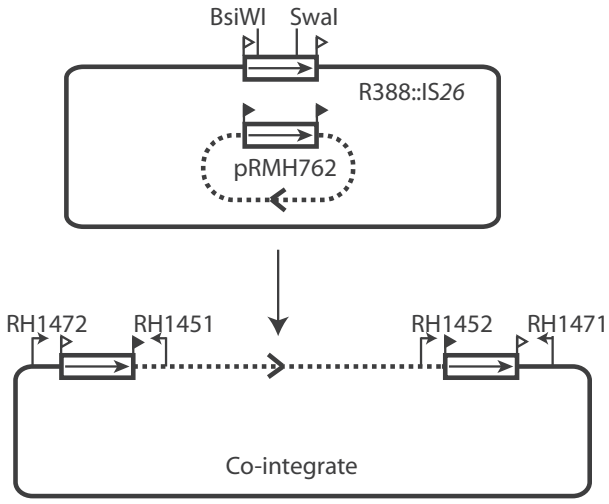

FIG 5 Targeted cointegrate formation between R388::IS*26* and pRMH762. Open boxes are IS*26*s, and the horizontal arrows indicate the position and orientation of *tnp26*. Open flags denote the 8-bp direct repeat of bases 26745 to 26752 in R388 (GenBank accession no. BR000038). Solid flags denote the 8-bp direct repeat flanking Tn*4352*B in GenBank accession no. KF976462. The locations of primers used to map targeted cointegrates are shown. Note that the figure is not to scale.

tern, indicating that the IS*26* in R388::IS*26* remained the preferred target.

To perform the reciprocal experiment, a frameshift was introduced into the *tnp26* gene of R388::IS*26* at the position of the SwaI site in Fig. 2, to generate R388::IS*26*-FS–R producing an inactivated Tnp26. Cointegrates were formed between pRMH762 and R388::IS*26*-FS–R at a frequency of 1.8×10^{-6} cointegrates per transconjugant (Table 1), and this is similar to that seen between pRMH962 (IS*26*-FS-L) and R388::IS*26*. Again, mapping of five independent cointegrates produced the same restriction pattern. However, cointegrate formation was not detected when the participating plasmids were pRMH962 (IS*26*-FS-L) and R388::IS*26*-FS–R, both of which contain an IS with a frameshift in *tnp26* (Table 1), confirming the requirement for Tnp26.

Does only one end of IS*26* participate in the reaction? One possible way in which the targeting could be achieved is if Tnp26 preferentially binds to one end of IS*26* and the recombination reaction occurs at that end of the IS. In the experiments using a plasmid containing a frameshift in the *tnp26* gene of only one IS*26* copy, it was possible to use unique features introduced during the generation of the frameshifts to explore this possibility by determining the origin of each IS*26* (L and R in Fig. 5) in each cointegrate. In R388::IS*26*-FS–R, the unique SwaI site of IS*26* (Fig. 2) has been removed, and both of the IS*26*s in 10 independent cointegrates recovered from pRMH762 recombination with R388::IS*26*-FS–R were amplified by PCR and digested with SwaI. In 7 of the 10 cointegrates tested, the intact IS*26* was located on the left (Fig. 5) and the IS*26* containing a frameshift was located on the right. In the remaining cointegrates, the opposite was observed.

In pRMH962, digestion at the BsiWI site (Fig. 2) followed by end filling and religation generated a unique SnaBI site (TAC GTA) at bases 116 to 121 of the mutant IS*26* that is not present in the intact IS*26*. The two IS*26*s in 10 independent cointegrates recovered from crossing pRMH962 with R388::IS*26* were PCR amplified, and the products were digested with SnaBI. In 6 out of the 10 cointegrates tested, the intact IS*26* was located on the left and the IS*26* containing the frameshift was located on the right. In the remaining cointegrates, the locations were reversed. Hence, the reaction does not appear to occur at one end of the IS.

Transfer of a TU. The experiments thus far have shown targeted incorporation of the IS*26*-containing plasmid pRMH762, which is essentially acting as a TU. Our model of IS*26*-mediated mobilization of resistance genes predicts that a TU should be able to form from an IS*26*-flanked structure and insert adjacent to another IS*26*. To detect TU movement, pRMH761 (Fig. 6A), which is the parent of pRMH762 and contains Tn*4352*B (IS*26*-*aphA1a*-IS*26*) conferring resistance to kanamycin and neomycin (Km^r Nm^r), was introduced into DH5α with R388::IS*26*. While Ap^r Km^r Tp^r cointegrates would be recovered if the complete pRMH761 was incorporated into R388::IS*26*, incorporation of only the TU should generate Km^r Tp^r cointegrates that are ampicillin susceptible (Ap^s) (Fig. 6B). Km^r Tp^r transconjugants were recovered, and among 100 colonies tested, only one was Ap susceptible. Three further Ap^s Km^r Tp^r transconjugants were recovered from two additional experiments.

Mapping confirmed that in plasmids recovered from these transconjugants, Tn*4352*B now replaced the single IS*26* in R388::IS*26*. Recovery of this transposon-like structure (Tn*4352*B) is indicative of movement of only one IS*26* and the *aphA1*-containing segment. Plasmid DNA from these transconjugants was also amplified with the R388 backbone primers RH1471 and RH1472 combined with primers aphA1-F and aphA1-R internal to *aphA1a* (see Fig. 6B for primer locations), and the sequences of the products confirmed that the *aphA1a*-containing TU (TU*aphA1a*) had been inserted adjacent to the IS*26* in R388::IS*26*. Again, the two IS*26*s were in direct orientation separated by the unique portion of the incoming TU*aphA1a*, and no further duplication of the target sequence had occurred. An amplicon of 3.4 kb was generated with primers RH1471/RH1472, demonstrating that only a single copy of the TU had inserted adjacent to the IS*26* (Fig. 6B).

Ap^r Tp^r transconjugants were also screened for growth on media containing kanamycin to distinguish Km^r cointegrates with the complete pRMH761 incorporated (Fig. 6D1 and D2) from Km^s ones with only the equivalent of pRMH762 (Fig. 6C). Of the 100 Ap^r Tp^r cointegrates examined, 43 were also resistant to kanamycin (Km^r). Mapping of 10 Ap^r Km^r Tp^r cointegrates revealed that the incoming plasmid was next to the preexisting IS*26* in R388::IS*26*, and both D1 (6) and D2 (4) configurations were formed. The greater abundance of the Ap^r Tp^r Km^s product compared to R388::Tn*4352*B may be explained if the *aphA1a* TU can excised from pRMH761 to yield pRMH762, which can replicate, and the free form of TU*aphA1a*, which cannot replicate. It is also possible that TU*aphA1a* can be excised from the cointegrates D1 and D2 formed with R388. Further work will be needed to explore this.

The DDE residues of Tnp26 are required for activity. A conserved DDE motif in IS*6* family transposases was predicted by Mahillon and Chandler (2), and alignments between the Tnp26 and the transposases of other family members confirmed that they are conserved in this family. This amino acid triad coordinates divalent metal cations, making it essential for activity. However, these residues have not been shown to be essential for Tnp26 activity. The codons for the aspartic acid (D) residues at positions 82 and 142 of Tnp26 and the glutamic acid (E) residue at position 177

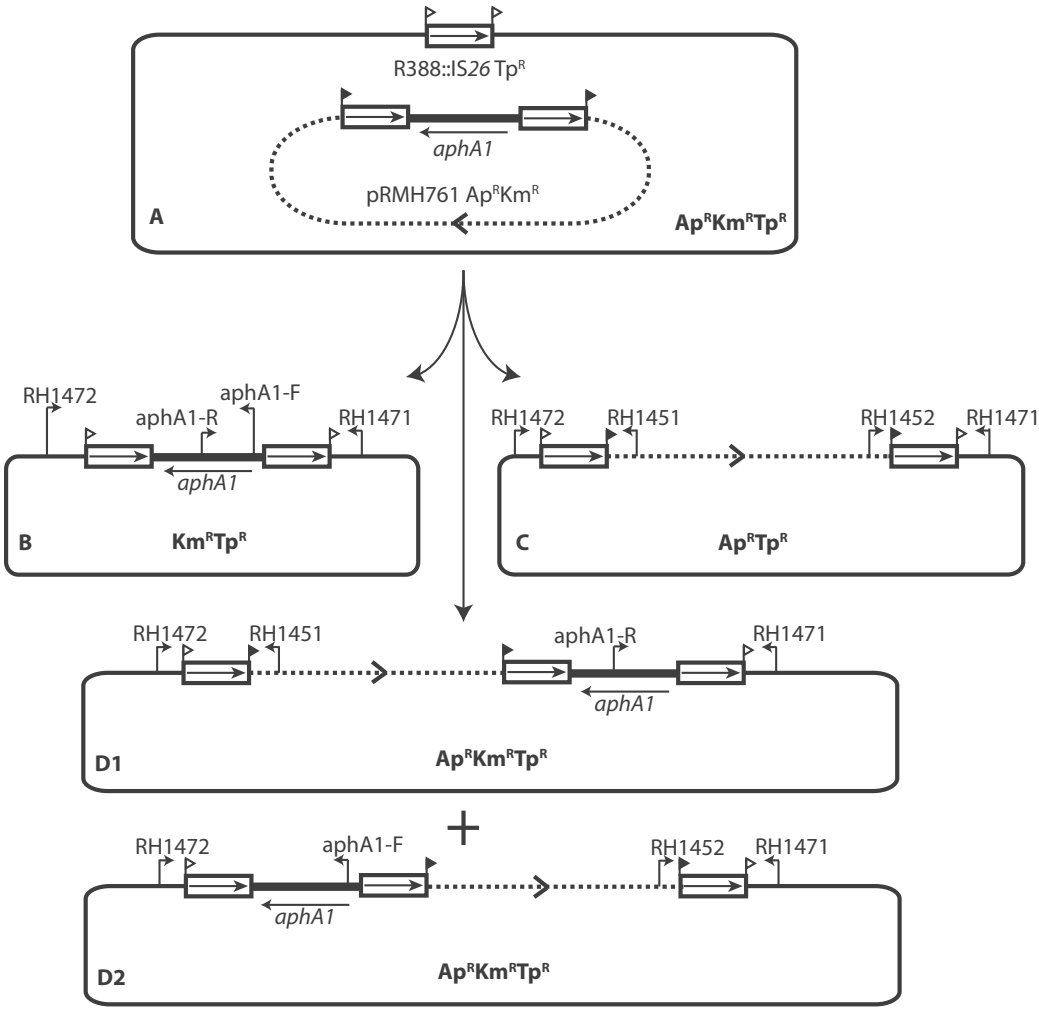

FIG 6 Direct transfer of a TU from pRMH761 into R388::IS*26*. The reaction between the two plasmids in the donor cell (A) should form four possible products (B to D). (B) TU*aphA1* alone incorporated into R388::IS*26*. (C and D) cointegrates formed between R388::IS*26* and pRMH762 (C) or the complete pRMH761 (D1 and D2). IS*26*s are shown as open boxes, with an arrow indicating the orientation of *tnp26*. Open flags denote the 8-bp direct repeat of bases 26745 to 26752 in R388 (GenBank accession no. BR000038). Solid flags denote the 8-bp direct repeat flanking Tn*4352*B in GenBank accession no. KF976462. The location of primers used to map targeted cointegrates is shown by bent arrows. The phenotypes of recipient cells containing the plasmids shown are also indicated, and Tp^r strains are also Su^r. Note that the figure is not to scale.

were altered in the IS*26*-containing plasmid pRMH977 (Ap^r), causing a leucine substitution. The clones generated, pRMH987, pRMH988, and pRMH989, respectively, were each tested for the ability to form cointegrates with the conjugative plasmid R388. No Ap^r Sm^r Tp^r colonies were recovered from three independent determinations for each clone (Table 2), which is indicative of the inability to form cointegrates when any residue of the DDE motif is altered. However, the parent plasmid pRMH977 formed cointegrates with R388 at a very low frequency (25-fold lower than pRMH762). A higher frequency of 2.14×10^{-4} cointegrates per transconjugant was obtained with R388::IS*26*. When the derivatives of pRMH977 producing Tnp26 with LDE, DLE, or DDL were tested with R388::IS*26* (Table 2), the cointegration frequency of 6.4×10^{-6} to 8.4×10^{-6} was about 25-fold lower and equivalent to that of the *tnp26* frameshift mutant, pRMH978, which formed 8.35×10^{-6} cointegrates per transconjugant. Hence, the DDE residues are essential for Tnp26 activity.

DISCUSSION

The model presented here for the movement of IS*26* together with a unique DNA segment explains how regions containing several copies of IS*26* interspersed with different DNA segments containing antibiotic resistance genes or other genes arise. It also explains how the configuration of the tandem duplications that have been reported (Fig. 1B) are likely to have arisen. Moreover, the predictions of the model were able to be verified experimentally. Consequently, there are two distinct modes of movement for IS*26*. The first is cointegrate formation with duplication of the IS*26* and generation of a target duplication, and the second is TU incorporation at an existing IS*26* (Fig. 7). This feature is presumably shared by other members of the IS*6* family, setting this IS family apart from other IS with DDE transposases.

An intriguing aspect of the results presented here is the finding that a cointegrate with identical features is the end product of both low-frequency IS*26* transposition (when only one participating

TABLE 2 Transposition frequencies of DDE mutants

Plasmid	IS*26*	Target	Transposition frequency[a]		
			Mean	No.[b]	Range
pRMH977	IS*26*	R388	1.7×10^{-7}	3	5.1×10^{-8}–3.7×10^{-7}
pRMH978	IS*26*-FS-L[c]	R388	$<1.8 \times 10^{-8}$	3	$<1.1 \times 10^{-8}$–$<1.9 \times 10^{-8}$
pRMH987	IS*26* D82L	R388	$<5.3 \times 10^{-8}$	3	$<4.3 \times 10^{-8}$–$<7.1 \times 10^{-8}$
pRMH988	IS*26* D142L	R388	$<3.4 \times 10^{-9}$	3	$<2.8 \times 10^{-9}$–$<4.2 \times 10^{-9}$
pRMH989	IS*26* E177L	R388	$<4.4 \times 10^{-8}$	3	$<1.8 \times 10^{-8}$–$<5.9 \times 10^{-8}$
pRMH977	IS*26*	R388::IS*26*	2.1×10^{-4}	3	1.9×10^{-4}–2.4×10^{-4}
pRMH978	IS*26*-FS-L[c]	R388::IS*26*	8.4×10^{-6}	3	7.3×10^{-6}–9.2×10^{-6}
pRMH987	IS*26* D82L	R388::IS*26*	6.4×10^{-6}	3	4.8×10^{-6}–9.6×10^{-6}
pRMH988	IS*26* D142L	R388::IS*26*	6.4×10^{-6}	3	3.5×10^{-6}–1.1×10^{-5}
pRMH989	IS*26* E177L	R388::IS*26*	9.7×10^{-6}	3	4.3×10^{-6}–2.0×10^{-5}

[a] Transposition frequency expressed as cointegrates per transconjugant.
[b] Number of independent determinations.
[c] IS*26*-FS-L is an IS*26 tnp26* frameshift mutant.

molecule carries an IS) and high-frequency transposition (when both participating molecules carry an IS) (Fig. 7). The DDE residues of Tnp26 were clearly essential for both types of transposition activity. Although precisely how the conservative Tnp26-catalyzed reaction seen here is performed remains to be worked out and evidence for TU excision is needed, it is clear that IS*26* differs from all of the ISs examined in detail to date (2, 36).

We have also demonstrated the introduction of Tn*4352*B into R388 via a multistep process that requires the initial formation of R388 carrying IS*26* and either excision of the TU*aphA1a* prior to its incorporation or excision of pRMH762 from a cointegrate. This provides the first evidence for TU formation in a RecA-independent manner. A recent report also observed RecA-independent incorporation of an IS*26*-bla_{SHV} TU into pACYC184 carrying IS*26* but not into pACYC184 (30). However, details such as the Tnp26 dependence have not been reported, and the excision step requires more detailed investigation.

It seems likely that our model will also apply to other ISs in the IS*6* family, such as IS*257* (also known as IS*431*) and IS*1216*, both of which are associated with the mobilization of antibiotic resistance genes (37, 38). IS*257* (39) is of particular interest granted its role in the dissemination of resistance genes in staphylococci (40, 41). IS*257* has been shown to be active and to duplicate itself and create an 8-bp target when only one participating molecule contains the IS, but it reacts conservatively when both participants carry IS*257* (41). Although the strains used were not recombination deficient and a role for Tnp257 is implied rather than proven, these observations support the general applicability of the model within the IS*6* (IS*26*) family.

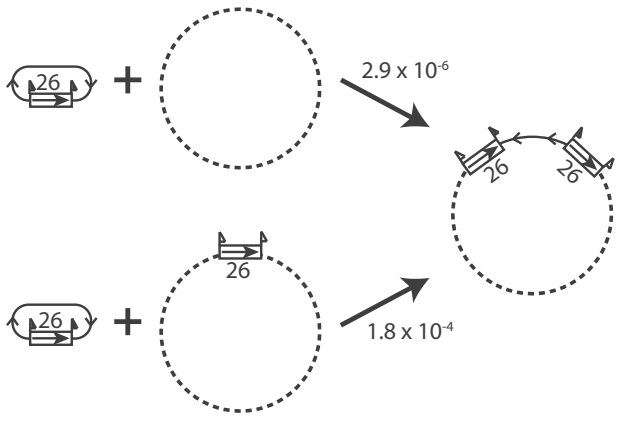

FIG 7 Two routes to cointegrate formation: random and targeted. The IS*26*s (boxes with an arrow indicating the orientation of the *tnp26* gene) in both plasmids are flanked by an 8-bp duplication indicated by a raised arrowhead (solid for the small plasmid and open for R388::IS*26*). The frequency of cointegrate formation is indicated on the arrows (cointegrates/transconjugant).

MATERIALS AND METHODS

Bacterial strains and media. *Escherichia coli* DH5α (*supE44* Δ*lacU169* [ϕ80 *lacZ*ΔM15] *hsdR17 recA1 endA1 gyrA96 thi-1 relA1*) was used to propagate plasmids. *E. coli* UB1637 (*lys his trp lac recA* Sm^r) was used as a recipient in transposition experiments. Bacteria were routinely cultured at 37°C in Luria-Bertani (LB) medium or on LB agar. Mueller-Hinton agar was used to select for resistance to trimethoprim. Antibiotics (Sigma) were added at the indicated concentrations: ampicillin, 100 μg ml^{-1}; kanamycin, 50 μg ml^{-1}; nalidixic acid, 25 μg ml^{-1}; streptomycin, 25 μg ml^{-1}; and trimethoprim, 25 μg ml^{-1}.

DNA manipulation. Plasmid DNA was isolated by alkaline lysis (11). DNA was digested with restriction enzymes according to the manufacturer's instructions, and fragments were separated through 0.7% agarose (Bioline) in 1 × Tris-acetate-EDTA (TAE) buffer. The size standards were a 1-kb ladder and λ DNA-HindIII (New England Biolabs).

PCRs were performed as previously described (11). The sequences for all primers used in this study are listed in Table 3. PCR products were purified for sequencing via gel extraction using an EconoSpin DNA column (Epoch Life Sciences). Routine sequencing was performed at the Australian Genome Research Facility (Sydney).

Cloning was performed as previously described (11), with minor modifications. All ligations were performed at a 3:1 M ratio of insert to vector with 40 U of T4 DNA ligase (New England Biolabs) in a final concentration of 1× ligase buffer. Chemically competent *E. coli* DH5α cells were prepared using a $CaCl_2$ method, and transformation was performed via heat shock.

Plasmid construction. The plasmids used in this study are listed in Table 4. pRMH762 is an Ap^r Km^s derivative of pRMH761 recovered after growth without kanamycin selection. It retains a single copy of IS*26* surrounded by a duplication of 119447 to 119454 bp in GenBank accession no. KF976462. pRMH761 (Ap^r Km^r Nm^r) has been described previously (12) and consists of an 8.8-kb BamHI fragment from pRMH760 (bases 117841 to 126672 in GenBank accession no. KF976462) containing Tn*4352*B (Km^r Nm^r) cloned into pUC19 (Ap^r). An IS*26* transposase knockout was generated by digesting pRMH762 with BsiWI, unique to the IS*26* (Fig. 2), followed by end filling with T4 DNA polymerase and religation. This introduced a 4-bp duplication of bases 114 to 117 relative

TABLE 3 Primers used in this study

Primer	Sequence (5′→3′)
RH1451[a]	TTCGGTGGATCCACCCAGATACGGCTGATGTC
RH1452[a]	CACACGGGATCCTTCGTTCCTGGTCGATTTTC
RH1453	TCGATAGATTGTCGCACCTG
RH1454	CTGCCTCGGTGAGTTTTCTC
RH1456[b]	GTGGCACATG**CTT**GAAACCTACGTGAAG
RH1457[b]	CTTCACGTAGGTTTC**AAG**CATGTGCCAC
RH1458[c]	CAACGTGATT**CTA**TGCGATCATGG
RH1459[c]	CCATGATCGCA**TAG**AATCACGTTG
RH1471	CCGCTCCAAAAACTATCCAC
RH1472	ATCGGAAATGGTTGTGAAGC
RH1476[b]	GATTCATCAACACG**TTG**AAAGCGCCGCC
RH1477[b]	GGCGGGCGCTTTC**AAC**GTGTTGATGAATC
aphA1-F	CAACGGGAAACGTCTTGCTC
aphA1-R	ATTCGTGATTGCGCCTGAG

[a] Underlined sequence indicates BamHI restriction site incorporated into the 5′ end of the primer.
[b] Bold sequence denotes modification to the template sequence to introduce a D→L amino acid substitution.
[c] Bold sequence denotes modification to the template sequence to introduce an E→L amino acid substitution.

to the left end of IS*26* (as shown in Fig. 2) and a frameshift in the *tnp26* gene leading to premature termination at a stop codon (bases 154 to 156 in IS*26*) forming a 30-aa protein. This form was designated IS*26*-FS-L, to indicate the location of the frameshift at the left-hand end of *tnp26*.

R388::IS*26*, an R388 derivative containing a single copy of IS*26*, was created from an R388::pRMH762 cointegrate via digestion with SwaI to excise the fragment located between the two IS*26*s followed by religation. R388::IS*26* contains a single IS*26* with an 8-bp duplication of bases 26745 to 26752 in R388 (GenBank accession no. BR000038). A frameshift was introduced into the *tnp26* gene in R388::IS*26* by digesting plasmid DNA with SwaI (Fig. 2) and treating it with 5 U of exonuclease III for 30 s to remove a small number of bases. Then the DNA was treated with 10 U of mung bean nuclease for 30 min at 30°C to generate blunt ends. The DNA was religated and transformed into chemically competent *E. coli* DH5α cells. Purified DNA was prepared from five transformants and digested with SwaI to confirm that the SwaI site had been removed by the exonuclease treatment. One transformant was selected, and sequencing of the amplicon generated by primers RH1471 and RH1472 revealed a 13-bp deletion in *tnp26*, removing bases 624 to 636 relative to the left end of IS*26*. This causes a frameshift at aa 186 in Tnp*26*, leading to a 187-aa protein, designated IS*26*-FS–R, to indicate its position near the 3′-end of *tnp26*.

As pRMH762 (9,656 bp) is too large to use with available site-directed mutagenesis kits, a smaller derivative, pRMH977 (3,695 bp), was constructed by amplifying and recloning the IS*26* from pRMH762. The IS*26* together with bases 119362 to 119454 and 122137 to 122225 from GenBank accession no. KF976462 was amplified with primers RH1451 and RH1452, which contain a BamHI site at their 5′ ends, to facilitate cloning into BamH1-digested, phosphatase-treated pUC19 vector. The size and orientation of inserts were determined in 10 transformants by digestion with PstI and NdeI. A transformant with the insert in the same orientation as pRMH762 (*tnp26* facing toward the pUC19 P_{lac}) (pRMH977), and a transformant with the insert in the opposite orientation (pRMH979) were retained. The codons for the DDE residues (Fig. 2) predicted to be conserved (2), were substituted in pRMH977 using a QuikChange II site-directed mutagenesis kit (Agilent Technologies) according to the manufacturer's instructions. The two aspartic acid residues at positions 82 and 142, and the glutamic acid residue at position 177 in Tnp*26* were changed to a leucine residue via site-directed mutagenesis using primer pairs RH1456/RH1457, RH1476/RH1477, and RH1458/RH1459 to generate clones pRMH987, pRMH988, and pRMH989, respectively. The amino acid substitution was confirmed by PCR amplification of IS*26* and sequencing.

Transposition assays. Strains for transposition assays were generated via conjugation of either R388 (Su^r Tp^r) or R388::IS*26* (Su^r Tp^r) into *E. coli* DH5α cells containing the nonconjugative plasmid pRMH762 (Ap^r) or pRMH977 (Ap^r) or one of their derivatives. Cointegrate formation was assessed by mating these strains with UB1637 (Sm^r) and selecting for Ap^r Sm^r Tp^r colonies. Transposition frequency was calculated as the number of Ap^r Tp^r transconjugants (cointegrates) per Tp^r Sm^r transconjugant (R388 or R388::IS*26*).

To determine the positions of cointegrate junctions in the R388 backbone, plasmid DNA isolated from two colonies from each of 10 independent transposition experiments was digested overnight with BsiWI and BglII. The presence of a BsiWI site in each IS*26* and two BsiWI and BglII sites in the R388 backbone allowed the determination of the approximate location of cointegrate formation between R388 and the IS*26*-containing plasmid. Targeted cointegrate formation in R388::IS*26* was detected by restriction mapping as described above, combined with a PCR mapping strategy that linked the DNA originating from the IS*26*-containing plas-

TABLE 4 Plasmids used in this study

Plasmid	Description	Resistance phenotype[a]	Reference
R388	IncW plasmid	Su Tp	42
R388::IS*26*	R388 with IS*26*[b]	Su Tp	This study
R388::IS*26*-FS–R	R388::IS*26* frameshift mutant[c]	Su Tp	This study
pRMH761	8.8-kb BamHI fragment of pRMH760 cloned into pUC19	Ap Km Nm	12
pRMH762	pRMH761 Km^s derivative[d]	Ap	This study
pRMH962	pRMH762 *tnp26* FS-L mutant[e]	Ap	This study
pRMH977	pRMH762 derivative[f,g]	Ap	This study
pRMH978	pRMH977 *tnp26* FS-L mutant[e]	Ap	This study
pRMH979	pRMH762 derivative[f,h]	Ap	This study
pRMH987	pRMH977 Tnp26 mutant D82L	Ap	This study
pRMH988	pRMH977 Tnp26 mutant D142L	Ap	This study
pRMH989	pRMH977 Tnp26 mutant E177L	Ap	This study

[a] Ap, ampicillin; Km, kanamycin; Nm, neomycin; Su; sulfamethoxazole; Tp, trimethoprim.
[b] IS*26* 8-bp duplication of bases 26745 to 26752 in R388 (GenBank accession no. BR000038).
[c] Lacks 13 bp (bases 624 to 636 from the left end of IS*26*, as shown in Fig. 5).
[d] Loss of *aphA1* and one IS*26* after overnight growth without kanamycin selection.
[e] Frameshift generated by end filling the BsiWI site and duplicating 116 to 119 bp from the left end of IS*26* as shown in Fig. 5.
[f] IS*26* together with bases 119362 to 119454 and 122137 to 122225 from GenBank accession no. KF976462.
[g] Cloned insert in the same orientation as pRMH762, with *tnp26* facing toward P_{lac} in pUC19.
[h] Cloned insert in the opposite orientation to pRMH762, with *tnp26* facing away from P_{lac} in pUC19.

mid across each IS*26* into the R388 backbone using primer pairs RH1471/1452 and RH1472/RH1451.

ACKNOWLEDGMENTS

This work and Chris Harmer were supported by NHMRC project grant APP1032465.

We thank Sashindran Anantham for assistance with some experiments, Amy Cain for construction of pRMH962, and Sally Partridge for pRMH761.

REFERENCES

1. **Mollet B, Iida S, Shepherd J, Arber W.** 1983. Nucleotide sequence of IS*26*, a new prokaryotic mobile genetic element. Nucleic Acids Res. **11:** 6319–6330.
2. **Mahillon J, Chandler M.** 1998. Insertion sequences. Microbiol. Mol. Biol. Rev. **62:**725–774.
3. **Trieu-Cuot P, Courvalin P.** 1984. Nucleotide sequence of the transposable element IS*15*. Gene **30:**113–120. http://dx.doi.org/10.1016/0378-1119(84)90111-2.
4. **Brown AM, Coupland GM, Willetts NS.** 1984. Characterization of IS*46*, an insertion sequence found on two IncN plasmids. J. Bacteriol. **159:** 472–481.
5. **Bräu B, Piepersberg W.** 1983. Cointegrational transduction and mobilization of gentamicin resistance plasmid pWP14a is mediated by IS*140*. Mol. Gen. Genet. **189:**298–303. http://dx.doi.org/10.1007/BF00337820.
6. **Nies BA, Meyer JF, Wiedemann B.** 1985. Tn*2440*, a composite tetracycline resistance transposon with direct repeated copies of IS*160* at its flanks. J. Gen. Microbiol. **131:**2443–2447.
7. **Wrighton CJ, Strike P.** 1987. A pathway for the evolution of the plasmid NTP16 involving the novel kanamycin resistance transposon Tn*4352*. Plasmid **17:**37–45. http://dx.doi.org/10.1016/0147-619X(87)90006-0.
8. **Colonna B, Bernardini M, Micheli G, Maimone F, Nicoletti M, Casalino M.** 1988. The *Salmonella wien* virulence plasmid pZM3 carries Tn*1935*, a multiresistance transposon containing a composite IS*1936*-kanamycin resistance element. Plasmid **20:**221–231. http://dx.doi.org/10.1016/0147-619X(88)90028-5.
9. **Hall RM.** 1987. pKM101 is an IS*46*-promoted deletion of R46. Nucleic Acids Res. **15:**5479. http://dx.doi.org/10.1093/nar/15.13.5479.
10. **Allard JD, Gibson ML, Vu LH, Nguyen TT, Bertrand KP.** 1993. Nucleotide sequence of class D tetracycline resistance genes from *Salmonella ordonez*. Mol. Gen. Genet. **237:**301–305.
11. **Cain AK, Liu X, Djordjevic SP, Hall RM.** 2010. Transposons related to Tn*1696* in IncHI2 plasmids in multiply antibiotic resistant *Salmonella enterica* serovar Typhimurium from Australian animals. Microb. Drug Resist. **16:**197–202. http://dx.doi.org/10.1089/mdr.2010.0042.
12. **Partridge SR, Hall RM.** 2003. In34, a complex In5 family class 1 integron containing *orf513* and *dfrA10*. Antimicrob. Agents Chemother. **47:** 342–349. http://dx.doi.org/10.1128/AAC.47.1.342-349.2003.
13. **Sundström L, Jansson C, Bremer K, Heikkilä E, Olsson-Liljequist B, Sköld O.** 1995. A new *dhfrVIII* trimethoprim-resistance gene, flanked by IS*26*, whose product is remote from other dihydrofolate reductases in parsimony analysis. Gene **154:**7–14. http://dx.doi.org/10.1016/0378-1119(94)00905-8.
14. **Cain AK, Hall RM.** 2011. Transposon Tn*5393*e carrying an *aphA1*-containing transposon upstream of *strAB* does not confer resistance to streptomycin. Microb. Drug Resist. **17:**389–394. http://dx.doi.org/10.1089/mdr.2011.0037.
15. **Post V, Hall RM.** 2009. AbaR5, a large multiple antibiotic resistance region found in *Acinetobacter baumannii*. Antimicrob. Agents Chemother. **53:**2667–2671. http://dx.doi.org/10.1128/AAC.01407-08.
16. **Ford PJ, Avison MB.** 2004. Evolutionary mapping of the SHV beta-lactamase and evidence for two separate IS*26*-dependent *bla*SHV mobilization events from the *Klebsiella pneumoniae* chromosome. J. Antimicrob. Chemother. **54:**69–75. http://dx.doi.org/10.1093/jac/dkh251.
17. **Gilmour MW, Thomson NR, Sanders M, Parkhill J, Taylor DE.** 2004. The complete nucleotide sequence of the resistance plasmid R478: defining the backbone components of incompatibility group H conjugative plasmids through comparative genomics. Plasmid **52:**182–202. http://dx.doi.org/10.1016/j.plasmid.2004.06.006.
18. **Hordijk J, Bosman AB, van Essen-Zandbergen A, Veldman K, Dierikx C, Wagenaar JA, Mevius D.** 2011. *qnrB19* gene bracketed by IS*26* on a 40-kilobase IncR plasmid from an *Escherichia coli* isolate from a veal calf. Antimicrob. Agents Chemother. **55:**453–454. http://dx.doi.org/10.1128/AAC.00866-10.
19. **Norman A, Hansen LH, She Q, Sørensen SJ.** 2008. Nucleotide sequence of pOLA52: a conjugative IncX1 plasmid from *Escherichia coli* which enables biofilm formation and multidrug efflux. Plasmid **60:**59–74. http://dx.doi.org/10.1016/j.plasmid.2008.03.003.
20. **Kim EH, Aoki T.** 1994. The transposon-like structure of IS*26*-tetracycline, and kanamycin resistance determinant derived from transferable R plasmid of fish pathogen, *Pasteurella piscicida*. Microbiol. Immunol. **38:**31–38. http://dx.doi.org/10.1111/j.1348-0421.1994.tb01741.x.
21. **Miriagou V, Carattoli A, Tzelepi E, Villa L, Tzouvelekis LS.** 2005. IS*26*-associated In4-type integrons forming multiresistance loci in enterobacterial plasmids. Antimicrob. Agents Chemother. **49:**3541–3543. http://dx.doi.org/10.1128/AAC.49.8.3541-3543.2005.
22. **Lee KY, Hopkins JD, Syvanen M.** 1990. Direct involvement of IS*26* in an antibiotic resistance operon. J. Bacteriol. **172:**3229–3236.
23. **Doublet B, Praud K, Weill FX, Cloeckaert A.** 2009. Association of IS*26*-composite transposons and complex In4-type integrons generates novel multidrug resistance loci in *Salmonella* genomic island 1. J. Antimicrob. Chemother. **63:**282–289.
24. **Nigro SJ, Farrugia DN, Paulsen IT, Hall RM.** 2013. A novel family of genomic resistance islands, AbGRI2, contributing to aminoglycoside resistance in *Acinetobacter baumannii* isolates belonging to global clone 2. J. Antimicrob. Chemother. **68:**554–557. http://dx.doi.org/10.1093/jac/dks459.
25. **Szczepanowski R, Braun S, Riedel V, Schneiker S, Krahn I, Pühler A, Schlüter A.** 2005. The 120,592 bp IncF plasmid pRSB107 isolated from a sewage-treatment plant encodes nine different antibiotic-resistance determinants, two iron-acquisition systems and other putative virulence-associated functions. Microbiology **151:**1095–1111. http://dx.doi.org/10.1099/mic.0.27773-0.
26. **Haniford DB.** 2006. Transpososome dynamics and regulation in Tn*10* transposition. Crit. Rev. Biochem. Mol. Biol. **41:**407–424. http://dx.doi.org/10.1080/10409230600987415.
27. **Reznikoff WS.** 2008. Transposon Tn5. Annu. Rev. Genet. **42:**269–286. http://dx.doi.org/10.1146/annurev.genet.42.110807.091656.
28. **Bertini A, Poirel L, Bernabeu S, Fortini D, Villa L, Nordmann P, Carattoli A.** 2007. Multicopy *bla*OXA-58 gene as a source of high-level resistance to carbapenems in *Acinetobacter baumannii*. Antimicrob. Agents Chemother. **51:**2324–2328. http://dx.doi.org/10.1128/AAC.01502-06.
29. **Loli A, Tzouvelekis LS, Tzelepi E, Carattoli A, Vatopoulos AC, Tassios PT, Miriagou V.** 2006. Sources of diversity of carbapenem resistance levels in *Klebsiella pneumoniae* carrying *bla*VIM-1. J. Antimicrob. Chemother. **58:**669–672. http://dx.doi.org/10.1093/jac/dkl302.
30. **Zienkiewicz M, Kern-Zdanowicz I, Carattoli A, Gniadkowski M, Cegłowski P.** 2013. Tandem multiplication of the IS*26*-flanked amplicon with the *bla*(SHV-5) gene within plasmid p1658/97. FEMS Microbiol. Lett. **341:**27–36. http://dx.doi.org/10.1111/1574-6968.12084.
31. **McGann P, Courvalin P, Snesrud E, Clifford RJ, Yoon EJ, Onmus-Leone F, Ong AC, Kwak YI, Grillot-Courvalin C, Lesho E, Waterman PE.** 2014. Amplification of aminoglycoside resistance gene *aphA1* in *Acinetobacter baumannii* results in tobramycin therapy failure. mBio **5**(2): e00915-14. http://dx.doi.org/10.1128/mBio.00915-14.
32. **Iida S, Mollet B, Meyer J, Arber W.** 1984. Functional characterization of the prokaryotic mobile genetic element IS*26*. Mol. Gen. Genet. **198:** 84–89. http://dx.doi.org/10.1007/BF00328705.
33. **Mollet B, Iida S, Arber W.** 1985. Gene organization and target specificity of the prokaryotic mobile genetic element IS*26*. Mol. Gen. Genet. **201:** 198–203. http://dx.doi.org/10.1007/BF00425660.
34. **Trieu-Cuot P, Courvalin P.** 1985. Transposition behavior of IS*15* and its progenitor IS*15*-Δ: are cointegrates exclusive end products? Plasmid **14:** 80–89. http://dx.doi.org/10.1016/0147-619X(85)90034-4.
35. **Trieu-Cuot P, Labigne-Roussel A, Courvalin P.** 1983. An IS*15* insertion generates an eight-base-pair duplication of the target DNA. Gene **24:** 125–129. http://dx.doi.org/10.1016/0378-1119(83)90137-3.
36. **Siguier P, Gourbeyre E, Chandler M. 26** February 2014. Bacterial insertion sequences: their genomic impact and diversity. FEMS Microbiol. Rev. http://dx.doi.org/10.1111/1574-6976.12067.
37. **Rice LB, Carias LL.** 1998. Transfer of Tn5385, a composite, multiresistance chromosomal element from *Enterococcus faecalis*. J. Bacteriol. **180:** 714–721.
38. **Barile S, Devirgiliis C, Perozzi G.** 2012. Molecular characterization of a

novel mosaic *tet*(S/M) gene encoding tetracycline resistance in foodborne strains of *Streptococcus bovis*. Microbiology **158:**2353–2362. http://dx.doi.org/10.1099/mic.0.058206-0.

39. **Rouch DA, Skurray RA.** 1989. IS*257* from Staphylococcus aureus: member of an insertion sequence superfamily prevalent among gram-positive and gram-negative bacteria. Gene **76:**195–205. http://dx.doi.org/10.1016/0378-1119(89)90160-1.
40. **Firth N, Skurray RA.** 1998. Mobile elements in the evolution and spread of multiple-drug resistance in staphylococci. Drug Resist. Updat. **1:**49–58.
41. **Stewart PR, Dubin DT, Chikramane SG, Inglis B, Matthews PR, Poston SM.** 1994. IS*257* and small plasmid insertions in the mec region of the chromosome of *Staphylococcus aureus*. Plasmid **31:**12–20. http://dx.doi.org/10.1006/plas.1994.1002.
42. **Revilla C, Garcillán-Barcia MP, Fernández-López R, Thomson NR, Sanders M, Cheung M, Thomas CM, de la Cruz F.** 2008. Different pathways to acquiring resistance genes illustrated by the recent evolution of IncW plasmids. Antimicrob. Agents Chemother. **52:**1472–1480. http://dx.doi.org/10.1128/AAC.00982-07.